Magnetic and electronic characterization of quasi-one-dimensional La_3RuO_7

P. Khalifah
Department of Chemistry and Princeton Materials Institute, Princeton University, Princeton, New Jersey 08540

R. W. Erwin and J. W. Lynn
NIST Center for Neutron Research, National Institute of Standards and Technology, Gaithersburg, Maryland 20899

Q. Huang
NIST Center for Neutron Research, National Institute of Standards and Technology, Gaithersburg, Maryland 20899 and Department of Materials and Nuclear Engineering, University of Maryland, College Park, Maryland 20742

B. Batlogg
Bell Laboratories Lucent Technologies, Murray Hill, New Jersey 07974

R. J. Cava
Department of Chemistry and Princeton Materials Institute, Princeton University, Princeton, New Jersey 08540
(Received 27 April 1999)

The electronic and magnetic properties of La_3RuO_7 have been investigated. Its structure consists of corner-sharing RuO_6 octahedra arranged in one-dimensional chains with a Ru-O-Ru angle of 145°. The magnetic susceptibility shows Curie-Weiss behavior at 50–400 K with $\theta = -14$ K and an effective moment of $3.94\mu_B$/Ru atom. At lower temperatures (20–50 K), short-range antiferromagnetic order is observed. Neutron diffraction and magnetic susceptibility data show that long-range antiferromagnetic order exists below 20 K. A spin-flop transition is observed at applied fields greater than 1 T and temperatures below 17 K. Band structure calculations predict anisotropic electronic behavior and show that the ground state should be antiferromagnetic. [S0163-1829(99)05737-9]

INTRODUCTION

Ruthenium oxides have long been known to be good metallic conductors. A large number of metallic compounds and even a superconductor are found among the pyrochlore,[1–3] perovskite,[4,5] and Ruddlesden-Popper[6,7] phases known for ruthenium oxides. These conducting materials are based on networks of two-dimensionally or three-dimensionally interconnected RuO_6 octahedra sharing edges or corners. Electronically, one-dimensional (1D) materials are known to have interesting electronic and magnetic properties such as charge density waves[8,9] and spin-Peierls transitions,[10,11] and are not expected to be conducting at low temperatures. It is therefore of interest to consider what happens to the transport properties of ruthenium oxides in which the electrons are confined to a 1D network of ruthenium oxide octahedra.

Ruthenium oxides of formula L_3RuO_7 were previously known for L=Pr–Sm.[12] These structures contain isolated chains of corner-sharing RuO_6 octahedra. They are part of a larger family of chain compounds with the formula L_3MO_7 which form with 5+ metal cations, where M can be Nb,[13] Ta,[14] Sb,[14] Mo,[15] Re,[16] Ru,[17] and Ir.[18] The first three compounds contain d^0 metals and are therefore expected to be electronically and magnetically inert. The last four compounds cover d-electron configurations ranging from d^1 to d^4. Of the electronically active transition-metal compounds in this family, the only one to have its properties characterized in detail is La_3MoO_7.[15]

We have succeeded in synthesizing the lanthanum member La_3RuO_7, which allows us to study the magnetic properties of 1D ruthenium oxygen chains without having to consider the effects of rare-earth magnetism. La_3RuO_7 contains Ru in a d^3 configuration and is expected to have the largest spin (3/2) possible for $4d$ and $5d$ transition metals in this structure type. Classical spin behavior is expected for La_3RuO_7, unlike the quantum-mechanical-type spin interactions expected for $S=1/2$ Mo in La_3MoO_7. Here we report the transport properties and magnetic characterization of La_3RuO_7.

EXPERIMENT

The starting materials were La_2O_3 (Alfa, 99.99%) dried at 900 °C overnight and RuO_2 (Alfa, 99.95%) dried for 1 h at 700 °C. La_2O_3 and RuO_2 were mixed to give a La:Ru ratio of 3.35:1. Samples were heated for 24 h at 1000 °C and 24 h at 1100 °C with intermediate grindings. The powder was then pressed into a pellet and heated at 1250 °C under flowing O_2 for 1 or more days until the reaction was completed. The high lanthanum content of the mixture resulted in small amounts (~10%) of excess La_2O_3 present in samples. The excess La_2O_3 was found to be necessary to avoid the formation of competing La-Ru-O phases during the reaction. Phase formation and purity were determined by powder x-ray diffraction.

Powder neutron diffraction data were taken to study the magnetic ordering. Structural data were collected at the NIST Center for Neutron Research using the BT-1 32-

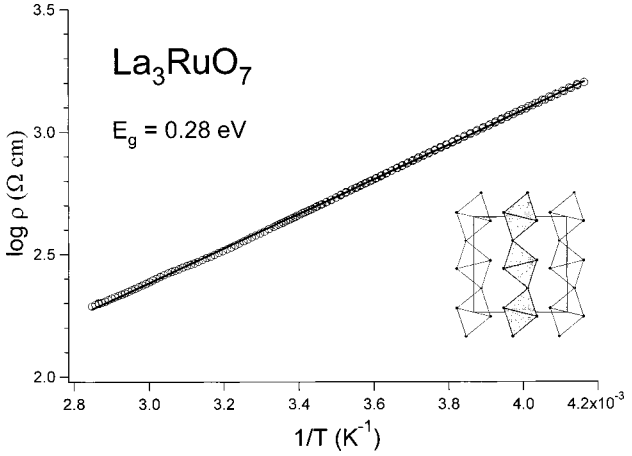

FIG. 1. Temperature dependence of the electrical resistivity of a polycrystalline sample of La_3RuO_7. The inset shows the chains of corner-sharing RuO_6 octahedra in La_3RuO_7 projected along *a*. The middle chain of the octahedra is displaced $(1/2)a$ perpendicular to the plane of the other two.

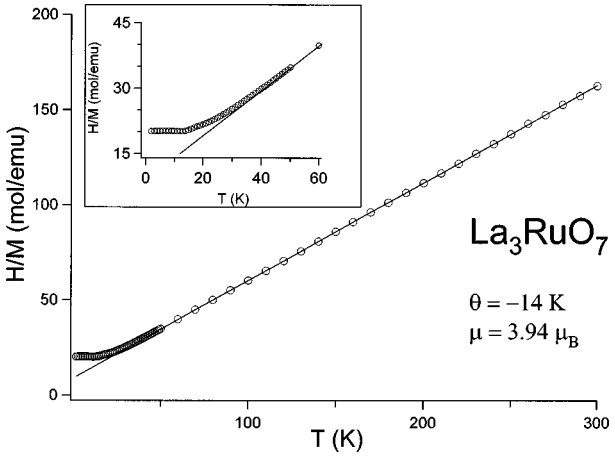

FIG. 2. Temperature dependence of the reciprocal magnetic susceptibility of La_3RuO_7 measured in a field of 0.1 T. The fit to the Curie-Weiss law is shown as a solid line. The inset shows an enlargement of low-temperature data.

counter high-resolution powder diffractometer. Neutrons of wavelength 2.0784 Å produced by a Ge (311) monochromator were used to collect data at 30 and 1.5 K. Intensities were measured in steps of 0.05° in the 2θ range of 3°–168°. The magnetic order parameter was measured using the BT-9 triple-axis spectrometer over the temperature range of 2–35 K using neutrons of wavelength 2.351 Å produced by a pyrolytic graphite (002) monochromator.

Measurements of ac resistivity were performed using the four-probe technique. Four copper leads were attached to sample bars (approximately $1\times1\times2\ mm^3$) using silver paint. Data were collected at 240–350 K. A superconducting quantum interference device (SQUID) magnetometer was employed to measure the magnetic properties of samples upon heating through temperatures of 2–400 K under fields of 0.01–5.5 T. Data were corrected for core diamagnetism.

The electronic band structure of La_3RuO_7 was calculated using the LMTO 47C program developed by Anderson and co-workers.[19,20] The program employs the linear muffin-tin orbital (LMTO) method within the tight-binding approximation. All relativistic effects except spin-orbit coupling were included in the calculations. Integrations over *k* space were performed using the tetrahedron method with a total of 105 irreducible *k* points.

RESULTS AND DISCUSSION

Our neutron diffraction data show that La_3RuO_7 has orthorhombic symmetry, *Cmcm*, with $a=11.2093(1)$ Å, $b=7.4617(1)$ Å, and $c=7.607\,71(8)$ Å. The ruthenium octahedra are organized into corner-sharing chains as seen in the inset to Fig. 1. The octahedra are nearly ideal, although the apical (shared) oxygen atoms are slightly displaced from the center of the basal plane, and the Ru-O apical bonds are 0.04 Å longer than the Ru-O bonds in the basal plane. The chain of corner-shared RuO_6 octahedra is highly buckled. The Ru-O-Ru angles in the chain are 145°, rather than the ideal 180° expected for a straight chain. Deviation from the 180° angle results in a decreased overlap between Ru *d* and oxygen *p* orbitals, and results in a decrease in electronic bandwidth. This reduced bandwidth results in a tendency for electron localization. In ruthenium-based pyrochlores, a bond angle of 133° between corner-shared octahedra is thought of as the minimum angle that will allow metallic behavior.[21] The chains are separated from each other by 7.46 Å in the [010] direction and 6.73 Å in the [110] direction, suggesting that interchain electronic and magnetic interactions will be weak. The details of the structure determination will be presented elsewhere.[22]

Measurements of the electrical resistivity of polycrystalline pellets (Fig. 1) showed La_3RuO_7 to be a thermally activated semiconductor with a band gap of 0.28 eV. A room-temperature resistivity of 425 Ω cm was observed. We can therefore conclude that the charge carriers are highly localized. The measured resistivity in a polycrystalline pellet necessarily includes both along-chain and across-chain contributions. However, the high value of the resistivity and the activated behavior indicates that the compound is semiconducting, even along the chain axis. Although one might expect the chains to be metallic based on the good conduction properties of ruthenium oxides and the 145° bond angle, it is not surprising to find that these chains are semiconducting. The 1D chains are much more vulnerable to defect scattering than the interconnected 3D network found in pyrochlores and perovskites.

The half-filling of the Ru t_{2g} band makes La_3RuO_7 a candidate Mott insulator. Semiconducting behavior has already been observed in the molybdenum[15] $(4d^1)$ and iridium[18] $(5d^4)$ analogs of this compound. In light of these results, it does not seem that electron-correlation-induced localization is the cause of the semiconducting behavior in the present case. The activation energy of La_3RuO_7 is somewhat higher than the value of 0.16 eV reported for La_3MoO_7 single crystals measured along the chain axis.[15] However, both the polycrystalline nature of La_3RuO_7 samples and the presence of small amounts of the highly insulating La_2O_3 make the value reported here merely an upper limit on the ruthenate resistivity.

The inverse magnetic susceptibility of samples measured for an applied field of 0.1 T showed Curie-Weiss behavior above 50 K (Fig. 2). A linear fit to the data gave an antifer-

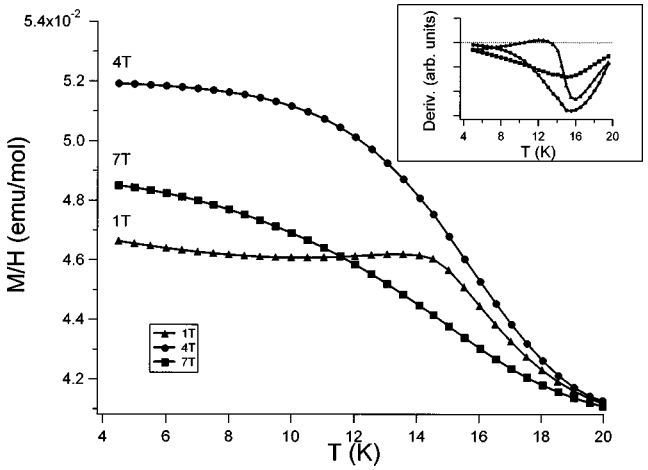

FIG. 3. Low-temperature M/H data for three applied fields (1, 4, and 7 T) taken on heating. Samples were field cooled. The inset shows $d(M/H)/dT$.

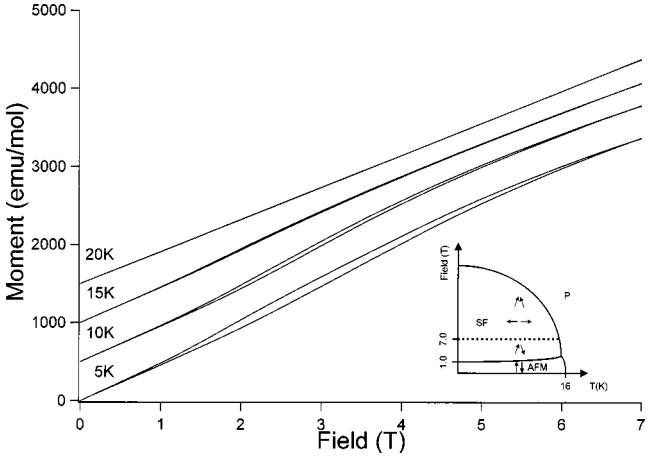

FIG. 4. Magnetic hysteresis loop for La_3RuO_7 at 5, 10, 15, and 20 K. Higher-temperature data are offset along the y axis. The inset shows a typical magnetic phase diagram for a system of weakly interacting spins undergoing a spin-flop transition. SF, spin-flop state; AFM, antiferromagnetic state; P, paramagnetic state. Observed temperature and fields boundaries are noted on the chart.

romagnetic θ value of -14 K. An effective moment of $3.96\mu_B$ per Ru atom was obtained, in good agreement with the expected spin-3/2 value of $3.87\mu_B$. Below 50 K, short-range antiferromagnetic correlations were observed, as seen in the deviation in the susceptibility from the Curie-Weiss fit line. The data measured at applied fields of 1–7 T were virtually identical in the range of 20–400 K.

Plotting the data as M/H vs T (Fig. 3) revealed field-dependent magnetic features below 20 K. At 5 K, the sample magnetization (per Ru atom) was $0.08\mu_B$ at 1 T, $0.37\mu_B$ at 4 T, and $0.60\mu_B$ at 7 T. For fields of $\leqslant 2$ T, a broad antiferromagnetic-type maximum was observed at 12 K. Samples measured at higher fields showed no such maximum. Instead, they showed a saturating magnetization curve. We conclude that the saturating magnetism is the result of the spin canting of an antiferromagnetically ordered lattice.

Because of the small moment, it was difficult to precisely assign the critical temperature (T_c) of the ordering transition from the plot of the M/H data. To assist in assigning the transition temperature, the derivative of M/H with respect to temperature was plotted (Fig. 3, inset). It can be seen that the derivative gradually decreases over the range of 20–16 K to its minimum at $\sim$16 K. We interpret this as evidence for a broad transition to the ordered state. The maximum of the transition shows a slight field dependence. As the field is increased from 1 to 7 T, the transition temperature gradually decreases from 16 to 15 K.

As the applied field was increased from 1 to 4 T, the values of M/H at temperatures below the transition temperature increased. However, applied fields in excess of 4 T caused a decrease in the values of M/H in this low-temperature regime. To investigate this further, the dependence of M on H was measured at 5, 10, 15, and 20 K (Fig. 4). At temperatures of 5–15 K the M vs H curves exhibit nonlinearity. At applied fields of less than 1 T, there is no hysteresis in the data, as would be expected for a typical antiferromagnetically ordered compound. Hysteresis was observed at applied fields greater than 1 T, consistent with the appearance of a small ferromagnetic moment. We interpret these data as evidence for a broad spin-flop transition at fields of $\sim$1 T, with the polycrystalline nature of the sample contributing to the broadening. A proposed phase diagram for this spin-flop transition is shown in the inset to Fig. 4. Although the most likely explanation for the observed behavior is a spin-flop transition, it is possible that a metamagnetic transition similar to that observed in rare-earth antimonides[23] is being observed.

The most accurate determination of the magnetic transitions came from neutron-scattering experiments. Figure 5(a) shows the magnetic scattering obtained by subtracting the 30 K data (a temperature well above the ordering temperature) from the data at 1.5 K (a temperature where the sample is in the magnetically ordered ground state).[24] Two relatively broad magnetic peaks [$\sim$0.55° full width at half maximum (FWHM)] were observed, demonstrating that three-dimensional magnetic ordering occurs at low temperatures. The magnetic peaks were much broader than the nuclear peaks (0.22° FWHM), indicating that the magnetic domains are small compared to the nuclear crystallite size. Since only two magnetic peaks were present, it was not possible to refine the antiferromagnetic structure.

The intensity of the higher-angle magnetic reflection was followed as a function of temperature in the vicinity of the phase transition temperature at zero applied magnetic field. A plot of the intensity of the magnetic reflection as a function of temperature is shown in Fig. 5(b). It can be unambiguously seen that long-range order is present below 19 K. The plot shows that the major ordering transition at 17 K is preceded by a gradual onset of ordering between 19 and 17 K. Both a Bragg-Williams fit (for an ideal ferromagnet) and a Bragg-Williams fit with crossover to a power law (to fit the broadened ordering transition) are shown superimposed on the data points.

The magnetic data provide insights into the dimensionality of La_3RuO_7. In a theoretical model for a 1D spin-3/2 Ising system, the maximum in the magnetic susceptibility will occur at $T_{max}=4.70\theta$.[25,26] Based on this result, we expect T_{max} to occur at 66 K if La_3RuO_7 is an electronically 1D material. However, a T_{max} of 12 K was observed at the lowest applied field studied. In addition, there can be no long-

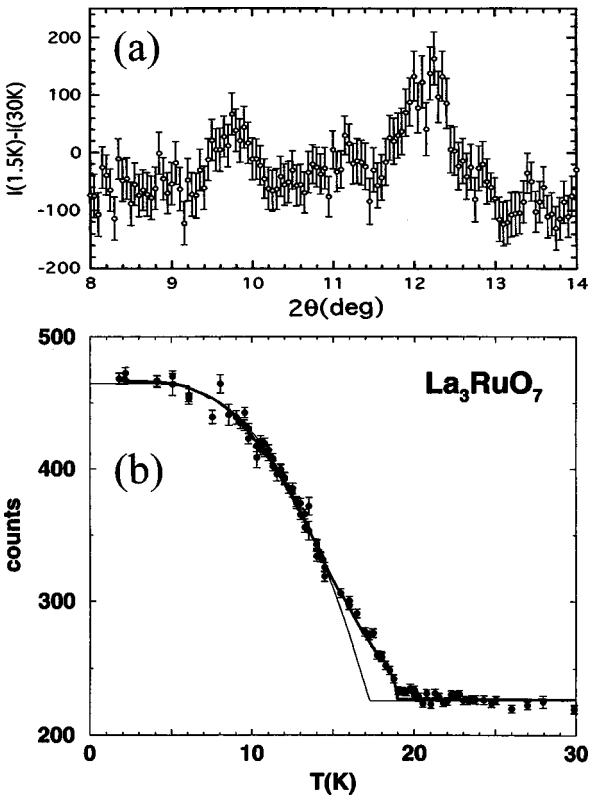

FIG. 5. (a) The difference of the neutron intensity data at 1.5 K from those at 30 K (data collected with $\lambda = 2.0784$ Å) shows two magnetic peaks at $d = 12.20$ Å ($2\theta = 9.77°$) and 9.80 Å ($2\theta = 12.17°$). (b) The intensity of the magnetic neutron diffraction peak at $d = 9.80$ Å in La_3RuO_7 as a function of temperature. The thin line is a fit at 2–18 K to the Brillouin function squared with $S = 0.61$ and $T = 17.38 \pm 0.12$ K. The thick line includes a crossover to a power law with S fixed at 0.5, T_c(Brillouin) = 17.67 K, T_c(power law) = 19.0 K, and $\beta = 0.315$.

range order in a 1D compound.[25] We can therefore conclude that the ruthenium spins are not behaving in a purely one-dimensional manner.

The relative energies of different spin alignments in La_3RuO_7 were obtained from LMTO calculations, as presented in Table I. The antiferromagnetic arrangement of spins studied consisted of antiparallel alignment of spins along the chains, but ferromagnetically aligned spins in the planes perpendicular to the chains. The antiferromagnetic (AFM) lattice required the symmetry of the monoclinic space group $A2m$, using an a-centered unit cell of $a = 7.608$ Å, $b = 11.209$ Å, and $c = 7.462$ Å with $\beta = 90°$ (this lattice has the same size as the original cell, but now the chains run parallel to the a axis). This unit cell has twice as many unique Ru sites as the original cell. Nonmagnetic and ferromagnetic (FM) calculations were also done in the $A2m$ space group to facilitate comparison of the ground-state energies. Both the FM and AFM ground states were lower in energy than the nonmagnetic ground state. Since the FM and AFM calculations differ only in their intrachain configuration, the lower energy of the AFM configurations allows us to conclude that the intrachain spin interactions are antiferromagnetic.

TABLE I. LMTO energies per unit cell ($La_{12}Ru_4O_{28}$).

Spin order	Energy (eV)	Relative energy (eV)
None	−12 069.1298	0.000
FM	−12 069.1562	−0.0264
AFM	−12 069.1657	−0.0359

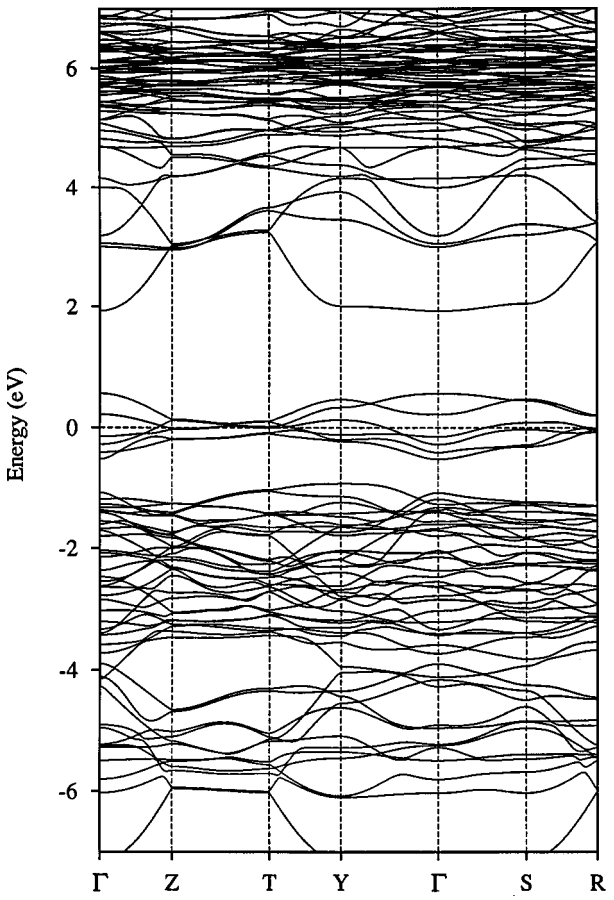

FIG. 6. The nonmagnetic band structure of La_3RuO_7. Symmetry directions are Γ (0,0,0), Z ($\frac{1}{2}$,0,0), T ($\frac{1}{2}$,1,0), Y (0,1,0), S (0,$\frac{1}{2}$,$\frac{1}{2}$), and R ($\frac{1}{2}$,$\frac{1}{2}$,$\frac{1}{2}$). In these calculations the chains run parallel to the a axis.

The results of the band structure calculations for the nonmagnetic ground state are presented in Fig. 6. The t_{2g} ruthenium orbitals at E_F and the e_g ruthenium orbitals 2 eV above E_F show similar momentum dependences. In the nonmagnetic calculation, the bands are flat along vectors perpendicular to the chains ($Z \rightarrow T$, $Y \rightarrow \Gamma$, $\Gamma \rightarrow S$) and are dispersive along vectors parallel to the chains ($\Gamma \rightarrow Z$, $T \rightarrow Y$, $S \rightarrow T$). This supports the characterization of La_3RuO_7 as a quasi-one-dimensional material. The maximum width of the six-electron t_{2g} band at E_F is only 1 eV. It is likely that this narrow band is at least part of the reason that La_3RuO_7 is semiconducting.

The results of partial density of states calculations allow us to label the peaks in the density of states (DOS) plot with their proper atomic character, as illustrated in Fig. 7(a). The t_{2g} and e_g bands arise from the interactions of the Ru d orbitals with the O(1) and O(3) p orbitals. The t_{2g} band is located at E_F and is rather narrow, while the e_g band is a broadband found at energies of 2–4 eV (relative to E_F). The O(2) atoms in the center of the La_4O tetrahedra show only

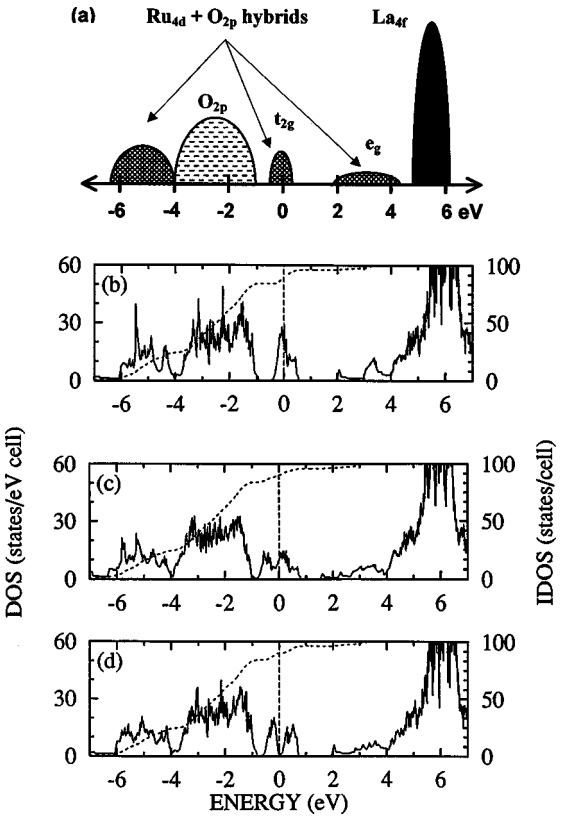

FIG. 7. The density of states for La_3RuO_7. A schematic of the levels is given in (a). The calculated results for nonmagnetic (b), FM (c), and AFM (d) ground states.

minute hybridization with the t_{2g} and e_g bands, supporting the conclusion that the O(2) atoms are not facilitating interchain interactions. The bulk of the oxygen *p*-orbital states occurs between -1 and -4 eV, although some additional hybrid Ru-O(1) and Ru-O(3) states occur at -4 to -6 eV. A large number of La $4f$ states are found at 5–6 eV. When we compare the DOS plots for the nonmagnetic [Fig. 7(b)] and magnetic [Figs. 7(c) and 7(d)] calculations for La_3RuO_7, we can see that the largest changes occur in the vicinity of E_F. In the absence of magnetism, there is a high density of states at E_F. In contrast, the density of states at E_F is partially reduced in the ferromagnetic configuration and is almost completely eliminated in the antiferromagnetic configuration.

CONCLUSIONS

Although the long-range ordering of La_3RuO_7 below 20 K prevents this material from being characterized as fully one dimensional, the measurements and calculations we have performed on this compound show that many of its features reflect its one-dimensional geometry. In particular, the semiconducting properties are a change from the good metallic behavior of 2D and 3D ruthenium networks and the antiferromagnetic transition does not have the sharp maximum that is expected from higher-dimensional spin lattices. The calculated Ru bands show that there is little orbital overlap in directions perpendicular to the chains.

We have found temperature- and field-dependent magnetic ordering in La_3RuO_7. Neutron-scattering data and plots of M/H vs T showed a canted antiferromagnetic arrangement of spins below 17 K, while the application of a field caused a temperature-dependent magnetic hysteresis to appear in M vs H plots due to a spin-flop transition. In light of the unusual magnetism also found with the strongly interacting spins in La_3MoO_7 ($\theta = -511$ K),[15] it seems that this low-dimensional structure type may enable numerous different types of magnetic configurations.

We have provided the initial characterization of an interesting $S = 3/2$ ruthenium compound. The presence of a complete series of $4d$ and $5d$ transition metals with band fillings of d^0–d^4 should allow a systematic investigation of the magnetism of heavy transition metals in this intriguing one-dimensional structure type.

ACKNOWLEDGMENT

This work was supported by the National Science Foundation Grant No. DMR-9725979.

[1] R. J. Bouchard and J. L. Gillson, Mater. Res. Bull. **6**, 669 (1971).
[2] H. Kobayashi, R. Kanno, Y. Kawamoto, T. Kamiyama, F. Izumi, and A. W. Sleight, J. Solid State Chem. **114**, 15 (1995).
[3] W. J. Zhu, S. T. Ting, and P. H. Hor, J. Solid State Chem. **129**, 308 (1997).
[4] R. J. Bouchard and J. F. Weiher, J. Solid State Chem. **4**, 80 (1972).
[5] M. Shepard, S. McCall, G. Cao, and J. E. Crow, J. Appl. Phys. **81**, 4978 (1997).
[6] Y. Maeno, H. Hasimoto, K. Yoshida, S. Nishizaki, T. Fujita, J. G. Bednorz, and F. Lichtenberg, Nature (London) **372**, 532 (1994).
[7] R. J. Cava, H. W. Zandbergen, J. J. Krajewski, W. F. Peck, Jr., B. Batlogg, S. Carter, R. M. Fleming, O. Zhou, and L. W. Rupp, Jr., J. Solid State Chem. **116**, 141 (1995).
[8] P. Monçeau, N. P. Ong, A. M. Portis, A. Meerschaut, and J. Rouxel, Phys. Rev. Lett. **37**, 602 (1976).
[9] J. Dumas, C. Schlenker, J. Marcus, and R. Buder, Phys. Rev. Lett. **50**, 757 (1983).
[10] M. Isobe and Y. Ueda, J. Phys. Soc. Jpn. **65**, 1178 (1996).
[11] J. P. Boucher and L. P. Regnault, J. Phys. I **6**, 1939 (1996).
[12] F. P. F. van Berkel and D. J. W. Ido, Mater. Res. Bull. **21**, 1103 (1986).
[13] A. Kanh-Harari, L. Mazerolles, D. Michel, and F. Robert, J. Solid State Chem. **116**, 103 (1995).
[14] H. J. Rossell, J. Solid State Chem. **27**, 115 (1979).
[15] J. E. Greedan, N. P. Raju, A. Wegner, P. Gougeon, and J. Padiou, J. Solid State Chem. **129**, 320 (1997).
[16] G. Wltschek, H. Paulus, I. Svoboda, H. Ehrenberg, and H. Fuess, J. Solid State Chem. **125**, 1 (1996).
[17] W. A. Groen, F. P. F. van Berkel, and D. J. W. Ijdo, Acta Crystallogr., Sect. C: Cryst. Struct. Commun. **43**, 2264 (1987).
[18] J. F. Vente and D. J. W. Ijdo, Mater. Res. Bull. **26**, 1255 (1991).

[19] O. K. Anderson and O. Jepsen, Phys. Rev. Lett. **53**, 2571 (1984).
[20] O. K. Anderson, Z. Pawlowska, and O. Jepsen, Phys. Rev. B **34**, 5253 (1986).
[21] K.-S. Lee, D.-K. Seo, and M.-H. Whangbo, J. Solid State Chem. **131**, 405 (1997).
[22] P. G. Khalifah, Q. Huang, and R. J. Cava, Mater. Res. Bull. (to be published).
[23] K. D. Myers, P. C. Canfield, V. A. Kalatsky, and V. L. Pokrovsky, Phys. Rev. B **59**, 1121 (1999).
[24] H. Zhang, J. W. Lynn, W.-H. Li, and T. W. Clinton, Phys. Rev. B **41**, 1129 (1990).
[25] L. J. de Jong and A. R. Miedema, Adv. Phys. **23**, 1 (1974).
[26] For a 1D Heisenberg spin-3/2 chain, $T_{max}=4.75\theta$ (Ref. 25).